

## Bulk silicon is susceptible to fatigue

Sanjit Bhowmick

*Ceramics Division, National Institute of Standards and Technology, Gaithersburg, Maryland 20899-8500, USA*

Juan José Meléndez-Martínez

*Departamento de Física, Universidad de Extremadura, 06071 Badajoz, Spain*

Brian R. Lawn<sup>a)</sup>

*Ceramics Division, National Institute of Standards and Technology, Gaithersburg, Maryland 20899-8500, USA*

(Received 12 September 2007; accepted 1 October 2007; published online 13 November 2007)

It has long been held that bulk silicon is immune from fatigue. We present contrary evidence demonstrating severe fatigue in macroscale cracks produced in cyclic loading of single-crystal silicon with a sphere indenter. The key ingredient is a component of shear stress acting on the cracks during contraction and expansion of the contact circle. This gives rise to frictional sliding at the crack walls, dislodging and ejecting slabs of material and debris onto the silicon surface. The damage expands with continued cycling, leading to progressive degradation of the surface. The results have implications concerning the function of silicon-based devices. © 2007 American Institute of Physics. [DOI: 10.1063/1.2801390]

It is well established experimentally<sup>1-5</sup> and theoretically<sup>6</sup> that silicon does not exhibit significant rate-dependent crack growth from chemical interactions with water or other environmental species. The conventional wisdom is that bulk silicon should therefore be immune from cyclic fatigue. Indeed, there appears to be no evidence in the fracture literature for fatigue effects in any form of bulk silicon—or in any other solid with the covalently bonded diamond structure for that matter—from conventional cyclic tests on machined tensile specimens with millimeter-scale planar cracks. Such immunity to long-lifetime degradation would clearly be of benefit in applications where periodic mechanical, electrical, or thermal stresses operate, e.g., sensor technology, electronic packaging, solar panels, and optical systems.<sup>5</sup>

On the other hand, studies over the past decade on small-scale micromachined silicon specimens have revealed clear evidence of stress-lifetime fatigue in high-cycle function, either compression-tension (especially) or tension-tension.<sup>3,7</sup> Microcrack flaws responsible for the fatigue in these specimens are characteristically of submicron dimensions. While the existence of substantial degradation is indisputable, there are conflicting schools of thought concerning the underlying mechanism: one school advocates intermittent crack extension by compression-assisted mechanical wedging of microscopic asperities or debris at the crack interface;<sup>3,7</sup> another school advocates extension by stress-assisted oxide formation-rupture.<sup>8-11</sup> Part of the reason for the continuing controversy is that it is not easy to observe the internal mechanisms of crack evolution at the submicron scale. It is argued that events at this level are unlikely to manifest themselves in macroscale fracture, in line with the notion that bulk silicon should remain fatigue resistant.<sup>8</sup>

In this study, we demonstrate the existence of pronounced fatigue in bulk silicon under cyclic loading with millimeter-scale spherical indenters. The resulting Hertzian contact stresses are generally intense because they are con-

centrated over small areas, and are strongly inhomogeneous.<sup>12</sup> In normal single-cycle contact, solids with the diamond-structure produce cone or ring cracks with imposed crystallographic features from preferred {111} cleavage.<sup>13,14</sup> Such cracks differ from those in traditional fracture specimens where they may be subjected to a significant component of shear as well as tensile loading.<sup>14</sup> Surface features at the crack interface—cleavage steps and debris—can act to hold the crack open on unloading, with characteristic residual surface displacements outside the ring circumference.<sup>15</sup> In tougher, heterogeneous polycrystalline ceramic materials, sphere contact can produce additional damage modes, including subsurface plasticity.<sup>12,16,17</sup> Such additional modes, when they do occur, are exacerbated in cyclic loading, leading to prominent mechanical degradation. However, plasticity is unlikely to be a factor in highly brittle, covalently bonded diamond-structure solids.<sup>15,18</sup> The question nevertheless arises: Are there other mechanisms of fatigue that might operate in bulk silicon, not detectable in traditional crack growth specimens or in tougher ceramics?

To address this question, cyclic contact tests at frequency 10 Hz were conducted on polished single-crystal (100) silicon plates using highly polished WC spheres of radius 1.6 mm—examination in a scanning electron microscope showed that the indenter surfaces had an asperity roughness of less than 1  $\mu\text{m}$ . We first determined that a critical load of  $550 \pm 25\text{N}$  (mean and standard deviation, 20 tests) was required to produce a ring crack on the as-polished silicon surface in single-cycle loading. Comparative single-cycle tests at 500N revealed no detectable crack traces or plastic slip lines on the indented surfaces, for hold times up to  $10^6$  s at peak load. This suggests an elastic response up to first ring fracture and confirms the absence of any moisture-assisted slow crack growth from surface flaws.<sup>2</sup> Bonded-interface section views through the contact center<sup>16</sup> revealed no subsurface plasticity in the silicon. However, a faint imprint of the asperity features on the WC sphere was apparent on

<sup>a)</sup>Electronic mail: brian.lawn@nist.gov

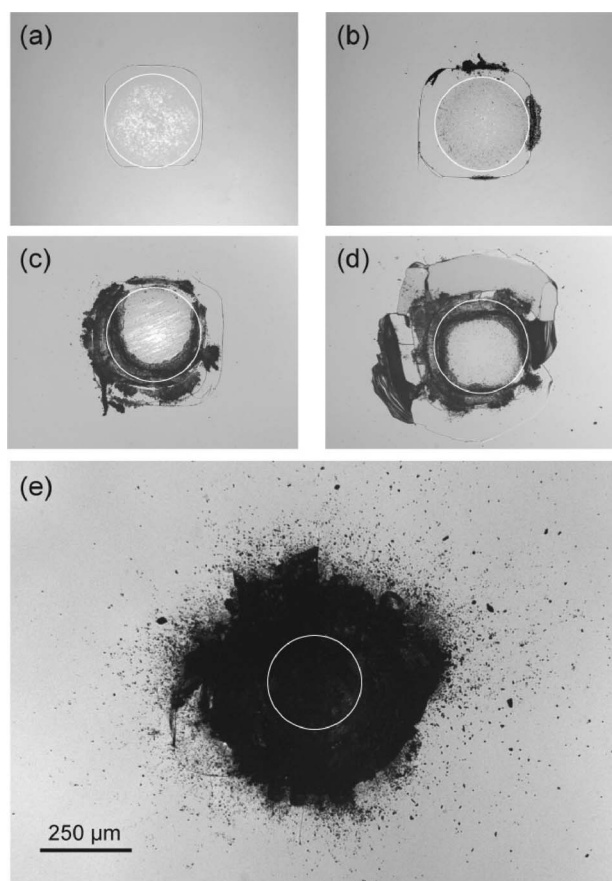


FIG. 1. Optical micrographs of contact damage in silicon (100), from cyclic loading of spherical indenter at  $P=250N$ : (a)  $n=1 \times 10^3$ , (b)  $n=5 \times 10^3$ , (c)  $n=20 \times 10^3$ , (d)  $n=85 \times 10^3$ , and (e)  $n=200 \times 10^3$  cycles.

the silicon surfaces, indicating spurious damage from the microcontacts.

Next, we made arrays of indentations at specified numbers of cycles  $n$  at contact load  $250N$ , i.e., less than one-half the critical load for fracture at  $n=1$ . Each cyclic test was interrupted to observe any surface damage. Figure 1 is a sequence of optical micrographs showing the evolution of such damage over hundreds of thousands of cycles. Each micrograph is a separate indentation. The white circle with diameter of  $\approx 260 \mu\text{m}$  artificially superimposed onto each micrograph indicates the contact circle computed from classical Hertzian elasticity theory.<sup>12</sup> Initially, the only sign of any surface damage is the contact imprint. At around  $n=10^3$  cycles, a faint ring crack abruptly appears [Fig. 1(a)]. The straight sides of this crack reflect the fourfold symmetry of the [100] monocrystal.<sup>14</sup> Generally, at least one side of the crack trace intersects the circle of contact, suggesting that the fracture has initiated from a flaw introduced by the contact itself. The observed asymmetry of the ring trace relative to the load axis is typical, attributable to a “pseudoinertia” as the crack circumvents the contact.<sup>19</sup> With further cycling, surface debris appears at the ring crack traces [Fig. 1(b)]. Continuation of cycling leads to intensification of debris formation, along with crack proliferation [Fig. 1(c)]. Still further cycling causes onset of chipping and detachment of collars of material outside the contact [Fig. 1(d)]. The removal of material accelerates until, ultimately, the indentation produces a “black hole” [Fig. 1(e)]. The existence of a pronounced fatigue damage process is palpable.

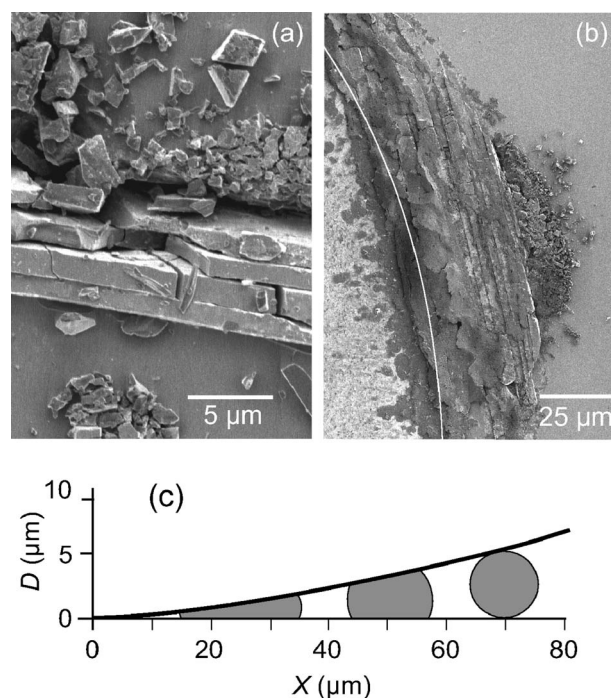


FIG. 2. Field emission scanning electron microscope images of ring crack segments in silicon (100). (a) Segment immediately outside contact at  $n=5 \times 10^3$ , showing platelet and particulate ejecta on surface. (b) Segment further outside contact at  $n=20 \times 10^3$ , showing smearing of ejecta. (c) Computed indenter-specimen displacement  $D$  as function of distance  $X$  outside elastic contact, showing how  $5 \mu\text{m}$  particles become trapped and crushed within gap.

Mechanistically, there appear to be two stages in the contact damage process. The first, precursor stage is associated with the development of the contact imprint. It is attributable to sliding within an annular region of the continuously expanding and contracting contact between two elastically mismatched bodies, resulting in superficial surface “fretting.”<sup>20</sup> Individual asperity microcontacts are capable of producing local plasticity.<sup>21</sup> In highly brittle solids such as silicon, the same microcontact damage provides nuclei for microcrack generation.<sup>22</sup> Such microcracks are believed to be the source of the ensuing ring crack initiation.

The second and more substantive stage in the damage process is the extensive degradation of the silicon surface after the onset of first ring cracking. Figure 2(a) shows scanning electron micrographs of one segment of a ring crack trace after  $n=5 \times 10^3$  cycles. This segment lies well outside the contact circle (out of field of view at bottom), so the crack is subject to some tensile opening.<sup>12</sup> Slabs and particulates of material, with minor dimensions up to  $5 \mu\text{m}$ , have been dislodged from within the crack walls and ejected onto the top surface. Particulate detritus in cyclic contact has previously been observed in tough polycrystalline ceramics, but there attributable to grain boundary sliding and attrition, exacerbated by moisture.<sup>12,17,23</sup> The appearance of debris here suggests analogous frictional sliding at the crack walls, associated with the small but not insignificant shear component alluded to earlier. The friction is attributable to the presence of steps and surface roughness that characterize the fracture of most brittle solids.<sup>17,24</sup> Platelets of material are then detached and squeezed out of the crack interfaces, akin to plate tectonics in earthquake faults. Repeated sliding of opposing crack walls and continued production of debris inevitably

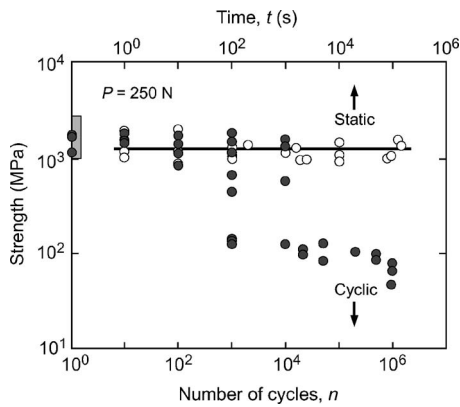


FIG. 3. Strength of silicon (100) plates after contact with spherical indenter as a function of number of cycles. Data shown for specimens with cyclic and static indentations. The box at the left is the mean and standard deviations for tests on unindented surface.

degrades the interfacial friction, thus magnifying surface displacements. This appears to be an altogether different kind of damage accumulation process than those envisaged by earlier groups working with small-scale specimens.<sup>5,7,8,11</sup>

With continued cycling, the ejected matter will protrude even higher relative to the surface outside the contact and thus become subject to crushing. Figure 2(b) shows the initial stages of this process at a multiple ring crack segment immediately outside the contact circle (white line) after  $20 \times 10^3$  cycles. Particulate matter closer to the contact has been smeared across the surface, somewhat obscuring underlying crack traces. Computation of the indenter/surface displacement  $D$  outside the contact circle was made using the Hertzian relation  $D(X) = (a^2/\pi r)[(\rho^2/a^2 - 1)^{1/2} + (\rho^2/a^2 - 2)\arctan(\rho^2/a^2 - 1)^{1/2}]$ , where  $X = \rho - a$  with  $a$  the elastic contact radius,  $r$  the indenter radius, and  $\rho$  the radial distance from the contact center.<sup>25</sup> As seen in Fig. 2(c), the calculated gap is narrow, so that micron-scale particulates are readily trapped and compressed. Ultimately, as crushed material is removed and the indenter penetrates into the specimen surface, the damage spreads and the indenter leaves the characteristic black hole.

Strength tests were then made to quantify the damage introduced into the indented surfaces, using a simple bilayer test configuration. Plates were loaded in biaxial flexure, indentations on the tensile side, and strengths calculated from the breaking loads.<sup>22</sup> All specimens broke from the contact site. Data for the strengths are plotted in Fig. 3 as a function of number of cycles  $n$ , along with data from comparative tests on specimens held at static peak load for an equivalent test duration. The box on the left axis indicates standard deviation bounds for unindented, as-polished surfaces. There is an indication of slight degradation in strength for indented relative to unindented surfaces in the immediate short-time region, suggesting that asperity flaws, while favored sites for crack nucleation, are only slightly more severe than those present in polished surfaces. However, whereas the strength data for static indentations show no detectable decline in strength over extended contact times (horizontal line), the corresponding cyclic data show a near order-of-magnitude decrement at first ring crack formation ( $n = 10^3 - 10^4$  cycles). Thereafter, the cyclic data decline only slowly, indicating limited continued downward crack extension with prolonged cycling—rather, the nature of the damage accumulation is

more one of damage proliferation and spreading into a lateral damage zone.

In summary, we have demonstrated the existence of pronounced cyclic fatigue in bulk silicon, from cracks on a near-millimeter scale. It might be argued that the Hertzian contact configuration used here is somewhat restrictive. While not necessarily implying universality of fatigue in silicon in all loading states, contact fields are nonetheless more representative of real complex mixed-mode loading states (e.g., in any functioning silicon device or component) than the plane tensile-crack tests used in traditional fracture mechanics testing. The essential ingredient is the existence of a shear component in the fracture process, with associated internal friction. Such a component is inevitable in crystallographically anisotropic solids such as monocrystalline silicon. The process may also apply to fine-grain polycrystalline materials in cyclic loading (polysilicon), as the stress field on the crack redistributes during contact contraction and expansion, causing wall-wall sliding during at least portion of the loading cycle. Whether the frictional sliding mechanism proposed here extends to microscale flaws—into the operational region of micromachined devices and microelectromechanical systems—is an intriguing question that remains to be resolved.

Certain equipment, instruments, or materials are identified in this paper in order to specify experimental details, and does not imply recommendation by the National Institute of Standards and Technology.

- <sup>1</sup>T. J. Chen and W. J. Knapp, *J. Am. Ceram. Soc.* **63**, 225 (1980).
- <sup>2</sup>B. R. Lawn, D. B. Marshall, and P. Chantikul, *J. Mater. Sci.* **16**, 1769 (1981).
- <sup>3</sup>H. Kahn, R. Ballarini, R. L. Mullen, and A. H. Heuer, *Proc. R. Soc. London, Ser. A* **455**, 3807 (1999).
- <sup>4</sup>E. D. Renuart, A. M. Fitzgerald, T. W. Kenny, and R. H. Dauskardt, *J. Mater. Res.* **19**, 2635 (2004).
- <sup>5</sup>R. F. Cook, *J. Mater. Sci.* **41**, 841 (2006).
- <sup>6</sup>T. A. Michalske and S. W. Freiman, *Nature (London)* **295**, 511 (1981).
- <sup>7</sup>H. Kahn, R. Ballarini, J. J. Bellante, and A. H. Heuer, *Science* **298**, 1215 (2002).
- <sup>8</sup>C. L. Muhlstein, E. A. Stach, and R. O. Ritchie, *Acta Mater.* **50**, 3579 (2002).
- <sup>9</sup>C. L. Muhlstein, E. A. Stach, and R. O. Ritchie, *Appl. Phys. Lett.* **80**, 1532 (2002).
- <sup>10</sup>P. Shrotriya, S. Allameh, S. Brown, Z. Suo, and W. O. Soboyejo, *Exp. Mech.* **43**, 289 (2003).
- <sup>11</sup>O. N. Pierron and C. L. Muhlstein, *Fatigue Fract. Eng. Mater. Struct.* **30**, 57 (2007).
- <sup>12</sup>B. R. Lawn, *J. Am. Ceram. Soc.* **81**, 1977 (1998).
- <sup>13</sup>S. Tolansky and V. R. Howes, *Proc. Phys. Soc. London, Sect. B* **70**, 521 (1957).
- <sup>14</sup>B. R. Lawn, *J. Appl. Phys.* **39**, 4828 (1968).
- <sup>15</sup>B. R. Lawn and H. Komatsu, *Philos. Mag.* **14**, 689 (1966).
- <sup>16</sup>B. R. Lawn, N. P. Padture, H. Cai, and F. Guiberteau, *Science* **263**, 1114 (1994).
- <sup>17</sup>N. P. Padture and B. R. Lawn, *J. Am. Ceram. Soc.* **78**, 1431 (1995).
- <sup>18</sup>Y.-W. Rhee, H.-W. Kim, Y. Deng, and B. R. Lawn, *J. Am. Ceram. Soc.* **84**, 561 (2001).
- <sup>19</sup>F. C. Frank and B. R. Lawn, *Proc. R. Soc. London, Ser. A* **299**, 291 (1967).
- <sup>20</sup>R. D. Mindlin, *J. Appl. Mech.* **16**, 259 (1949).
- <sup>21</sup>D. Tabor, *Hardness of Metals* (Clarendon, Oxford, 1951).
- <sup>22</sup>Y.-G. Jung, A. Pajares, R. Banerjee, and B. R. Lawn, *Acta Mater.* **52**, 3459 (2004).
- <sup>23</sup>S. Lathabai, J. Rödel, and B. R. Lawn, *J. Am. Ceram. Soc.* **74**, 1340 (1991).
- <sup>24</sup>J. S. Williams, B. R. Lawn, and M. V. Swain, *Phys. Status Solidi A* **2**, 7 (1970).
- <sup>25</sup>K. L. Johnson, *Contact Mechanics* (Cambridge University Press, London, 1985).